

JAERI-M

86-147

IMPROVED CONFINEMENT DURING
ICRF HEATING ON JFT-2M

October 1986

Hiroshi MATSUMOTO, Toshihide OGAWA, Hiroshi TAMAI,
Kazuo ODAJIMA, Mituru HASEGAWA*, Katsumichi HOSHINO
Satoshi KASAI, Hisato KAWASHIMA, Tomohide KAWAKAMI,
Tohru MATOBA, Toshiaki MATSUDA, Yukitoshi MIURA,
Masahiro MORI, Hiroaki OGAWA, Hideo OHTSUKA,
Seio SENGOKU, Tomoaki SHOJI, Norio SUZUKI,
Susumu TAKADA**, Yoshihiko UESUGI, Toshihiko YAMAUCHI,
and Takumi YAMAMOTO

日 本 原 子 力 研 究 所
Japan Atomic Energy Research Institute

JAERI-Mレポートは、日本原子力研究所が不定期に公刊している研究報告書です。
入手の問合わせは、日本原子力研究所技術情報部情報資料課（〒319-11 茨城県那珂郡東海村）あて、
お申しこしてください。なお、このほかに財団法人原子力弘済会資料センター（〒319-11 茨城県那珂郡
東海村日本原子力研究所内）で複写による実費領布をおこなっております。

JAERI-M reports are issued irregularly.
Inquiries about availability of the reports should be addressed to Information Division Department
of Technical Information, Japan Atomic Energy Research Institute, Tokaimura, Naka-gun, Ibaraki-
ken 319-11, Japan.

© Japan Atomic Energy Research Institute, 1986

編集兼発行 日本原子力研究所
印刷 日青工業株式会社

Improved confinement during ICRF heating on JFT-2M

Hiroshi MATSUMOTO, Toshihide OGAWA, Hiroshi TAMAI, Kazuo ODAJIMA, Mituru HASEGAWA*1, Katsumichi HOSHINO, Satoshi KASAI, Hisato KAWASHIMA, Tomohide KAWAKAMI, Tohru MATOBA, Toshiaki MATSUDA, Yukitoshi MIURA, Masahiro MORI, Hiroaki OGAWA, Hideo OHTSUKA, Seio SENGOKU, Tomoaki SHOJI, Norio SUZUKI, Susumu TAKADA*2, Yoshihiko UESUGI, Toshihiko YAMAUCHI, and Takumi YAMAMOTO.

Department of Thermonuclear Fusion Research
Naka Fusion Research Establishment
Japan Atomic Energy Research Institute
Naka-machi, Naka-gun, Ibaraki-ken

(Received September 22, 1986)

Significant improvement of energy confinement was observed on JFT-2M during ICRF heating. This improvement is associated with the sudden depression of H_{α}/D_{α} emission and the following increase of plasma stored energy, electron density and the radiation loss. This should be the same phenomena as H-mode transitions observed in ASDEX, PDX, and D-III divertor experiments with neutral beam injection heating. However, this transition is also observed in limiter discharges as well as in open divertor configurations on JFT-2M.

Keywords: JFT-2M, ICRF, H-mode, Divertor,

*1 On leave from Mitsubishi Electric Co.

*2 On leave from Mitsubishi Computer System Tokyo Co.

JFT-2MにおけるICRF加熱時のエネルギー閉じ込め改善現象

日本原子力研究所那珂研究所核融合研究部

松本 宏・小川 俊英・玉井 広史・小田島和男
長谷川 満^{*1}・星野 克道・河西 敏・川島 寿人
川上 知秀・的場 徹・松田 俊明・三浦 幸俊
森 雅博・小川 宏明・大塚 英男・仙石 盛夫
荘司 昭朗・鈴木 紀男・高田 晋^{*2}・上杉 喜彦
山内 俊彦・山本 巧

(1986年9月22日受理)

JFT-2MトカマクにおけるICRF加熱時に、プラズマ状態の遷移が起こり、エネルギー閉じ込めが著しく改善される現象が見出された。この遷移現象は、突然のH α /D α 信号の減少と、それともなう電子密度、放射損失の急な増加によって特徴づけられる。これは、他のASDEX, PDX, D-IIIなどの装置において観測されたHモードとよばれる現象と同じものである。しかし、これらの装置では、ダイバーター配位で、しかも、ダイバーター部から主プラズマへの中性粒子の逆流を減らした場合にのみ観測されている。JFT-2Mにおける実験では、極めて広範囲なプラズマ配位、形状で、この現象が観測されており、特に、リミター・プラズマでも、この遷移現象と、エネルギー閉じ込めの改善が見られている。

那珂研究所：〒311-02 茨城県那珂郡那珂町大字向山801-1

*1 三菱電気㈱

*2 三菱電気東部コンピュータシステム㈱

Contents

1. Introduction	1
2. Experimental arrangement	1
3. Experimental results	2
4. Discussion	6
5. Conclusion	7
Acknowledgement	7
References	8

目 次

1. 緒 言	1
2. 実験装置	1
3. 実験結果	2
4. 検 討	6
5. 結 び	7
謝 辞	7
参考文献	8

1. Introduction

Improvement of energy confinement during neutral beam heating with magnetic divertor configuration have been reported from several machines in these several years.^{1,2,3} These improved states are called H-mode state, and transitions from the normal, L-mode state usually take place after the sudden depression of H_{α} / D_{α} signals. These H-mode transitions have been mainly observed during neutral beam heating, and transition during ICRF heating was only reported from ASDEX experiment⁴⁾.

JFT-2M tokamak has a D shaped cross section, and it is capable of producing single null or double null open divertor configurations. However length between the null point and the divertor plate is less than 10 cm in normal operational conditions. And there is no throat nor a fan to suppress the back flow of neutral particles into a main plasma along the separatrix surface.

On JFT-2M, these suppression of H_{α} signals and also the following improvement of energy confinement have been observed with ICRF heating alone or with neutral beam injection heating alone. These transitions are observed under all kinds of JFT-2M operational mode, single null, double null open divertor configuration, and even limiter D-shaped plasma operation. There is no distinctive difference in the method of the heating as for the H-mode on JFT-2M.

Also threshold power of the additional heating for the transition to take place is very low under certain experimental condition. With ICRF heating, the smallest threshold power is about 200 kW, while ohmic input is about 250 kW.

2. Experimental arrangement

1. Introduction

Improvement of energy confinement during neutral beam heating with magnetic divertor configuration have been reported from several machines in these several years.^{1,2,3} These improved states are called H-mode state, and transitions from the normal, L-mode state usually take place after the sudden depression of H_{α} / D_{α} signals. These H-mode transitions have been mainly observed during neutral beam heating, and transition during ICRF heating was only reported from ASDEX experiment⁴⁾.

JFT-2M tokamak has a D shaped cross section, and it is capable of producing single null or double null open divertor configurations. However length between the null point and the divertor plate is less than 10 cm in normal operational conditions. And there is no throat nor a fan to suppress the back flow of neutral particles into a main plasma along the separatrix surface.

On JFT-2M, these suppression of H_{α} signals and also the following improvement of energy confinement have been observed with ICRF heating alone or with neutral beam injection heating alone. These transitions are observed under all kinds of JFT-2M operational mode, single null, double null open divertor configuration, and even limiter D-shaped plasma operation. There is no distinctive difference in the method of the heating as for the H-mode on JFT-2M.

Also threshold power of the additional heating for the transition to take place is very low under certain experimental condition. With ICRF heating, the smallest threshold power is about 200 kW, while ohmic input is about 250 kW.

2. Experimental arrangement

JFT-2M is a non-circular cross sectional machine with major radius of 131 cm. Minor radius of the machine is 59.5 cm in the vertical direction, and 41.5 cm in the major radius direction.

Three sets of high field side antennas are used in JFT-2M to launch fast wave in a two-ion hybrid resonance heating mode. Mixture of deuterium and hydrogen gas is used, and a hydrogen to deuterium density ratio is around 40% throughout the experiment. Plasma heating is achieved through electrons via Landau damping of ion-Bernstein wave which is converted from the fast wave at the thick mode conversion layer in the center of the machine, and high energy ions created by the heating is very small. Frequency of the wave is 16.8 MHz, which is the cyclotron frequency in 1.105 T of magnetic field. Toroidal magnetic field is from 1.2 to 1.25 T at the center of the plasma during the heating. The maximum RF power at the generator is 4.5 MW, however the maximum power coupled to the plasma is 2.2 MW with D-shaped limiter discharge, and 1.4 MW with the single null divertor configuration because of small loading impedance of antennas. In this paper we mean the RF heating power as the power radiated from the antenna into the torus.

Plasma stored energy is measured by both diamagnetic measurement and the magnetic probe measurement. JFT-2M has 24 magnetic probes in poloidal direction, and four saddle loops. $\beta_p + \alpha_i$ is calculated by the magnetic fitting code⁵⁾ from signals of these probes assuming six filament current in the plasma. The stored energies obtained from this fitting code, and the one from the diamagnetic measurement generally agree well. We mainly use fitting code results.

3. Experimental results

JFT-2M is a non-circular cross sectional machine with major radius of 131 cm. Minor radius of the machine is 59.5 cm in the vertical direction, and 41.5 cm in the major radius direction.

Three sets of high field side antennas are used in JFT-2M to launch fast wave in a two-ion hybrid resonance heating mode. Mixture of deuterium and hydrogen gas is used, and a hydrogen to deuterium density ratio is around 40% throughout the experiment. Plasma heating is achieved through electrons via Landau damping of ion-Bernstein wave which is converted from the fast wave at the thick mode conversion layer in the center of the machine, and high energy ions created by the heating is very small. Frequency of the wave is 16.8 MHz, which is the cyclotron frequency in 1.105 T of magnetic field. Toroidal magnetic field is from 1.2 to 1.25 T at the center of the plasma during the heating. The maximum RF power at the generator is 4.5 MW, however the maximum power coupled to the plasma is 2.2 MW with D-shaped limiter discharge, and 1.4 MW with the single null divertor configuration because of small loading impedance of antennas. In this paper we mean the RF heating power as the power radiated from the antenna into the torus.

Plasma stored energy is measured by both diamagnetic measurement and the magnetic probe measurement. JFT-2M has 24 magnetic probes in poloidal direction, and four saddle loops. $\beta_p + \alpha_i$ is calculated by the magnetic fitting code⁵⁾ from signals of these probes assuming six filament current in the plasma. The stored energies obtained from this fitting code, and the one from the diamagnetic measurement generally agree well. We mainly use fitting code results.

3. Experimental results

3-1 Improved confinement in a single null open divertor configuration

Figure 1 shows the H-mode transition in JFT-2M during ICRF heating with single null open divertor configuration. Time evolutions of L-mode discharge with the same discharge conditions are also superimposed in the figure by the narrow line. With the sudden depression of the H_{α}/D_{α} emission, radiation loss, and the electron density starts increasing rapidly. The time evolution of the ratio of the two line averaged electron densities measured vertically at $R=110$ cm and $R=124$ cm shown in the figure show that the electron density profile suddenly becomes broad with the onset of the transition. Plasma one turn voltage initially drops after the transition, however it soon starts increasing. Electron density, radiation loss, and plasma stored energy all drop after the sudden increase of H_{α}/D_{α} emission although the input of the RF heating power continues. Magnetic surface of the plasma just inside the separatrix surface is shown in Fig.2. Null point is represented by the cross in the figure. In this configuration, null point is in the bottom, and plasma surface is completely separated from the limiter surfaces.

Improvement of energy confinement is clearly shown by Fig.3 where global energy confinement times are plotted against the total heating power. L-mode values are represented by open circles and solid circles show the upper bound of the H-mode confinement time. Actually, after the transition, it increases from the L-mode value to the upper bound value accompanying the simultaneous increase of electron density.

3-2 Improved confinement in a double null open divertor configuration

Similar transitions were also observed with different plasma configurations. Figure 4 shows the outermost magnetic surface of the double

null open divertor configuration which has two null points in the top and bottom of the chamber. This is actually a limiter discharge, because the bottom null point is touching the divertor plate which is shown by vertical hatches in the figure, and the outermost surface is decided by the bottom divertor plates. Figure 5 shows the time evolutions of plasma parameter in this double null configuration. Transition takes place in a very similar way as the single null case. Although, after the onset of the transition, radiation loss and the electron density increase more rapidly than the single null case. This figure show the case with only single transition. However several transitions usually take place during 300 ms of the heating pulse.

3-3 Improved confinement in limiter discharges

Very much different from all the results of H-mode experiments on other machines, the transition also takes place with the pure limiter discharge in JFT-2M experiment. Figure 6 shows the outermost magnetic surface of the noncircular plasma, when the null points are completely outside of the vacuum vessel. In this case plasma surface is limited by the limiter on the inner side wall of the vessel. Transitions take place several times during the heating and time evolutions are shown in Fig.7. Depressions of H_{α}/D_{α} emission from the plasma periphery take place in all the poloidal positions at the same time. Radiation loss and the electron density increase very rapidly. Plasma stored energy determined by both the diamagnetic measurement and magnetic probe fitting calculation also increases after the transition, however it soon starts decreasing while the radiation loss and the electron density keep growing. Stored energy starts increasing again as soon as the radiation loss begins to decrease sharply with the sudden

increase of the H_{α}/D_{α} signals. Central electron temperature measured by soft x-ray pulse height analysis show the simultaneous increase with the stored energy. Plasma surface voltage also decrease with the increase of the stored energy.

Figure 8 show the comparison of this shot data with other "normal", L-mode heating results with the same plasma parameters and the same RF heating power in JFT-2M. In these figures, Fig.8(a) - (c) small open circles represent ohmic data, and solid circles are L-mode values. Transient behavior of #23810 shot data is shown by the two large circles showing the range of the change during the heating. In Fig.8(a), density dependence of global energy confinement time on the line average electron density is shown. It starts from the L-mode value and reaches the value very close to the ohmic value, and then goes back to the L-mode value with onset of the next transition. Increase of the stored energy during this transition is also shown in Fig.8-(b). Figure 8(c) show the maximum radiation loss when the stored energy is in the bottom, and the minimum radiation loss when the stored energy takes the maximum. At most about 70 - 75 % of the total input power is lost by the radiation. We still do not understand why this kind of transitions take place during the normal limiter discharges, however there are some prerequisite for this transitions. Without titanium gettering we do not see this, and as soon as we start titanium gettering we see this phenomena. Also we have to push plasma inward to limit plasma surface by the carbon limiter on the inner side of the vacuum vessel wall. We practically have several carbon limiters on the inner side wall, for each of three ICRF antennas has carbon side guards whose height from the wall is almost equal to that of guard limiters. They function as guard limiters.

4. Discussion

One of the most interesting features of improvement in energy confinement in JFT-2M ICRF heating is its dependence on the electron density. Stored energies of H-mode and L-mode shots with the same ICRF heating power and the discharge conditions, as well as the ohmic values are plotted against the line average electron density in Fig.9. H-mode values are represented by solid circles and L-mode values are by triangles and ohmic values are by open circles. In normal L-mode discharges in JFT-2M, incremental energy confinement time defined by $\tau_{ad} = \frac{\Delta W}{\Delta P}$ does not have density dependence.⁶⁾ Stored energy of ohmic discharge saturates above the critical density, around $4 \times 10^{19} \text{ m}^{-3}$. Stored energy with the same additional heating power also saturates above this density. However in H-mode discharge, it continues to increase with the electron density. These data are replotted in terms of the global energy confinement time in Fig.10. It keeps increasing with the electron density, and finally it reaches the maximum ohmic value. In this case, improvement of energy confinement may accompany improvement of particle confinement.

On the other hand, stored energy increases while the electron density decreases in transition cases with limiter discharge. Also there is the case in the single null open divertor configuration where stored energy maintains its H-mode values while the electron density and the radiation loss decline rapidly.

From these results, one may conclude that there are two modes in improvement of energy confinement in JFT-2M ICRF heating. One is the state, when energy confinement and the particle confinement improve at the same time. The other is the state when only energy confinement improves. In the

former case, radiation loss from the central part increases rapidly and the radiation loss profile becomes sharp. Also intensities of higher charge states metallic impurities increase more rapidly than the lower charge states emission. All these suggest the improvement of particle confinement results in accumulation of metallic impurities in the center of the plasma.

5. Conclusions

On JFT-2M, improvement of energy confinement, so called H-mode was observed with variety of plasma configurations, single null, or double null open divertor configuration, and D-shape limiter configuration during ICRF heating. Improvement of energy confinement usually accompanies improvement of particles, however there is the state where improvement of energy confinement does not accompany the improvement of particle confinement.

ACKNOWLEDGEMENT

The authors are very grateful to the members of the JFT-2M operation group for their excellent technical contributions. They are also indebted to Drs. S. Mori, K. Tomabechi, M. Tanaka, Y. Tanaka and A. Funabashi for their continuous encouragement.

former case, radiation loss from the central part increases rapidly and the radiation loss profile becomes sharp. Also intensities of higher charge states metallic impurities increase more rapidly than the lower charge states emission. All these suggest the improvement of particle confinement results in accumulation of metallic impurities in the center of the plasma.

5. Conclusions

On JFT-2M, improvement of energy confinement, so called H-mode was observed with variety of plasma configurations, single null, or double null open divertor configuration, and D-shape limiter configuration during ICRF heating. Improvement of energy confinement usually accompanies improvement of particles, however there is the state where improvement of energy confinement does not accompany the improvement of particle confinement.

ACKNOWLEDGEMENT

The authors are very grateful to the members of the JFT-2M operation group for their excellent technical contributions. They are also indebted to Drs. S. Mori, K. Tomabechi, M. Tanaka, Y. Tanaka and A. Funabashi for their continuous encouragement.

former case, radiation loss from the central part increases rapidly and the radiation loss profile becomes sharp. Also intensities of higher charge states metallic impurities increase more rapidly than the lower charge states emission. All these suggest the improvement of particle confinement results in accumulation of metallic impurities in the center of the plasma.

5. Conclusions

On JFT-2M, improvement of energy confinement, so called H-mode was observed with variety of plasma configurations, single null, or double null open divertor configuration, and D-shape limiter configuration during ICRF heating. Improvement of energy confinement usually accompanies improvement of particles, however there is the state where improvement of energy confinement does not accompany the improvement of particle confinement.

ACKNOWLEDGEMENT

The authors are very grateful to the members of the JFT-2M operation group for their excellent technical contributions. They are also indebted to Drs. S. Mori, K. Tomabechi, M. Tanaka, Y. Tanaka and A. Funabashi for their continuous encouragement.

REFERENCES:

1. KEILHACKER,M., and LACKNER,K., J.Nucl.Mater., 111 & 112(1982) 370.
2. SHIMADA,M., NAGAMI,M., IOKI,K., IZUMI,S., MAENO,M., MATSUDA,T.,
NISHIKAWA,M., OHTSUKA,M., SHINYA,K., YOKOMIZO,H., YOSHIDA,H.,
KITUNEZAKI,A., BROOKS,N., de RGASSIE,J., GROEBNER,R., and HSIEH,S.,
J.Nucl. Mater. 111 & 112 (1982) 362.
3. FONCK,R.J., BELL,M., BOL,K., BRAU,K., BUDNY,R., CECCHI,J.L., COHEN,S.,
DAVIS,S., DYLLA,H.F., GOLDSTON,R., GREK,B., HAWRYLUK,R.J.,
HIRSCHBERG,J., MANSFIELD,D., MCGUIRE,K., MUELLER,D., OASA,K.,
OKABAYSCHI,M., OWENS,D.K., RAMETTE,J., REEVES,R., REUSCH,M., SCHMIDT,G.,
SESNIC,S., SUCKEWER,S., TAKAHASHI,H., TENNEY,F., THOMAS,P., ULRICKSON,M.,
and YELLE,Y., J. Nucl. Mater., 111 & 112 (1982) 343.
4. STEINMETZ,K., WAGNER,F., WESNER,F., et. al.
Proc. of 13 th Europ. Conf. on Plasma Physics and Controlled Fusion
2(1986)21
5. SWAIN,D.W., and NEILSON,G.H., Nucl. Fusion, Vol.22, No.8 (1982) 1015
6. ODAJIMA,K., et. al. to be published in Phys. Rev. Let.

30667, 30656

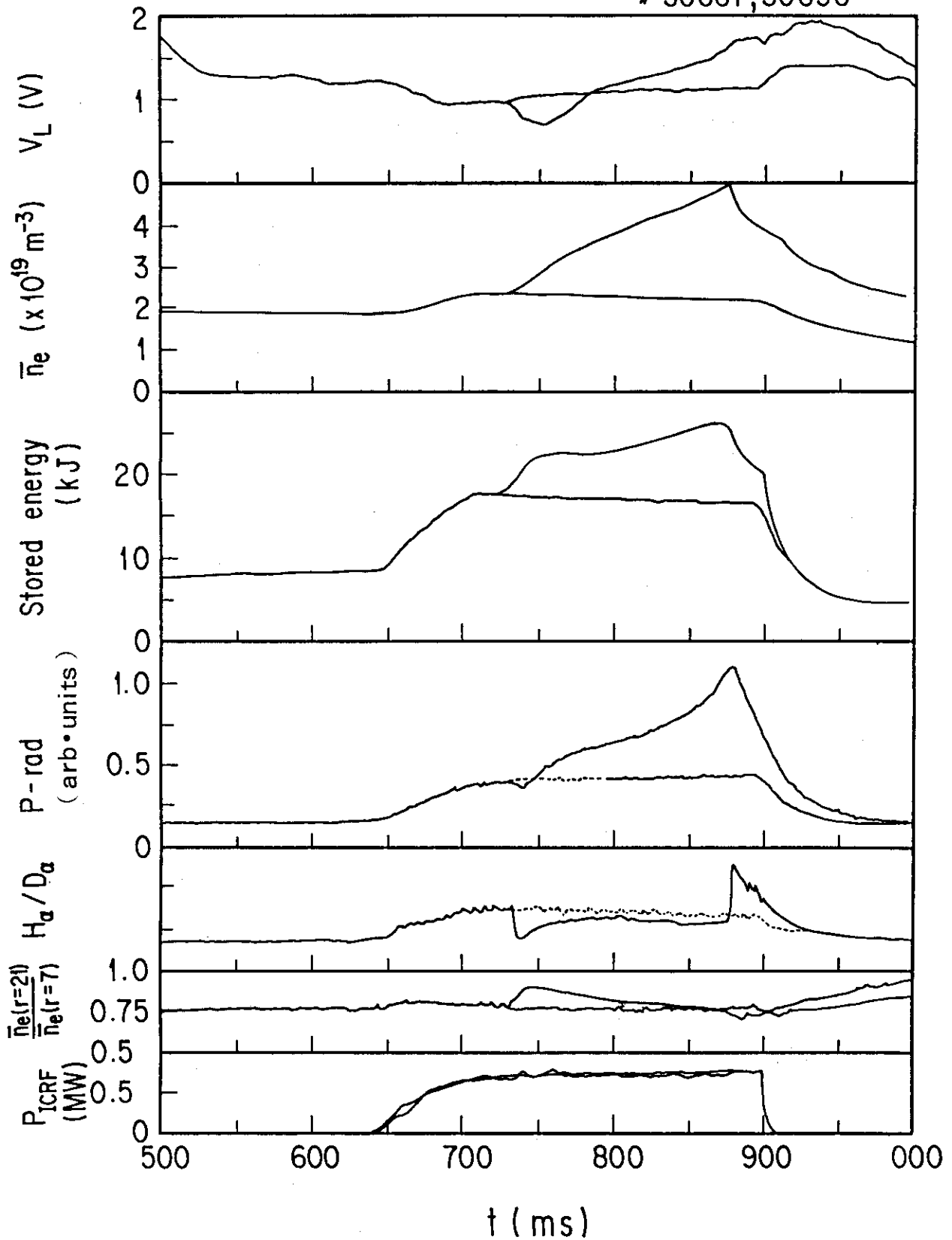
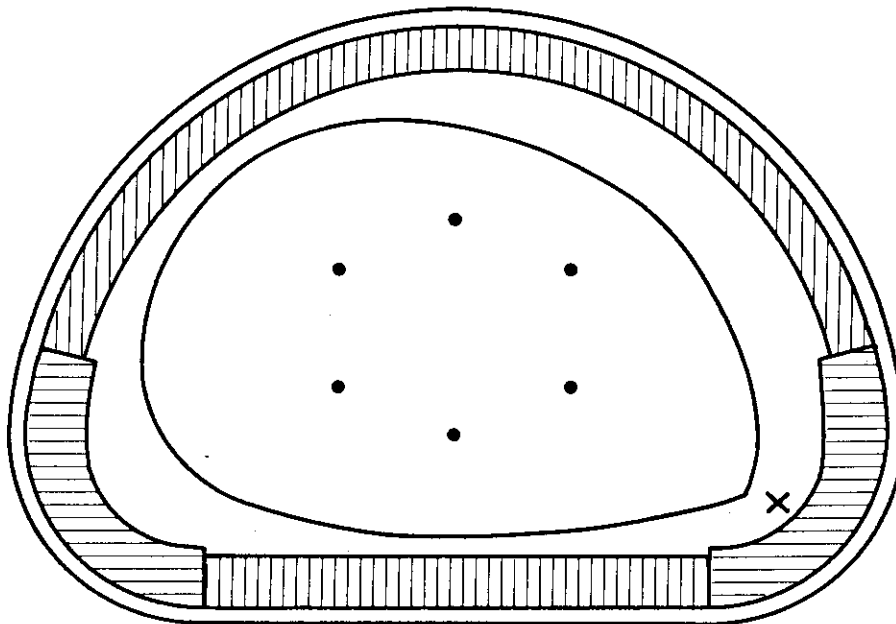


Fig.1 Time evolutions of one turn voltage, line averaged electron density, plasma stored energy, total radiation loss, emission of H_α/D_α , ratio of line averaged electron densities (measured vertically by FIR laser) at $R=151\text{cm}$ and at $R=137\text{cm}$, and ICRF heating power broadcasted from the antenna.

SHOT #30667



IP - CURRENT (KA)	254.8
R - AVERAGE (M)	1.294
Z - AVERAGE (M)	0.003
R - INNER (M)	0.996
R - OUTER (M)	1.580
Rj (M)	1.290
Zj (M)	0.027
A - HALF (M)	0.298
A - AVERAGE (M)	0.354
ELLIPTICITY	1.425
TRIANGULARITY	0.188
CROSS AREA (M**2)	0.394
VOLUME (M**3)	3.204
Q - SURF	3.730
BT (T)	1.264
BP + LI/2-1/2	0.390

Single null Divertor

Fig.2 Magnetic surface of the plasma just inside the separatrix surface is shown by the solid line. Null point is indicated by the cross. Positions of six filament current used for magnetic fitting code calculation are shown by the dots. Vertical hatches show the divertor plates and horizontal hatches show the guard limiter.

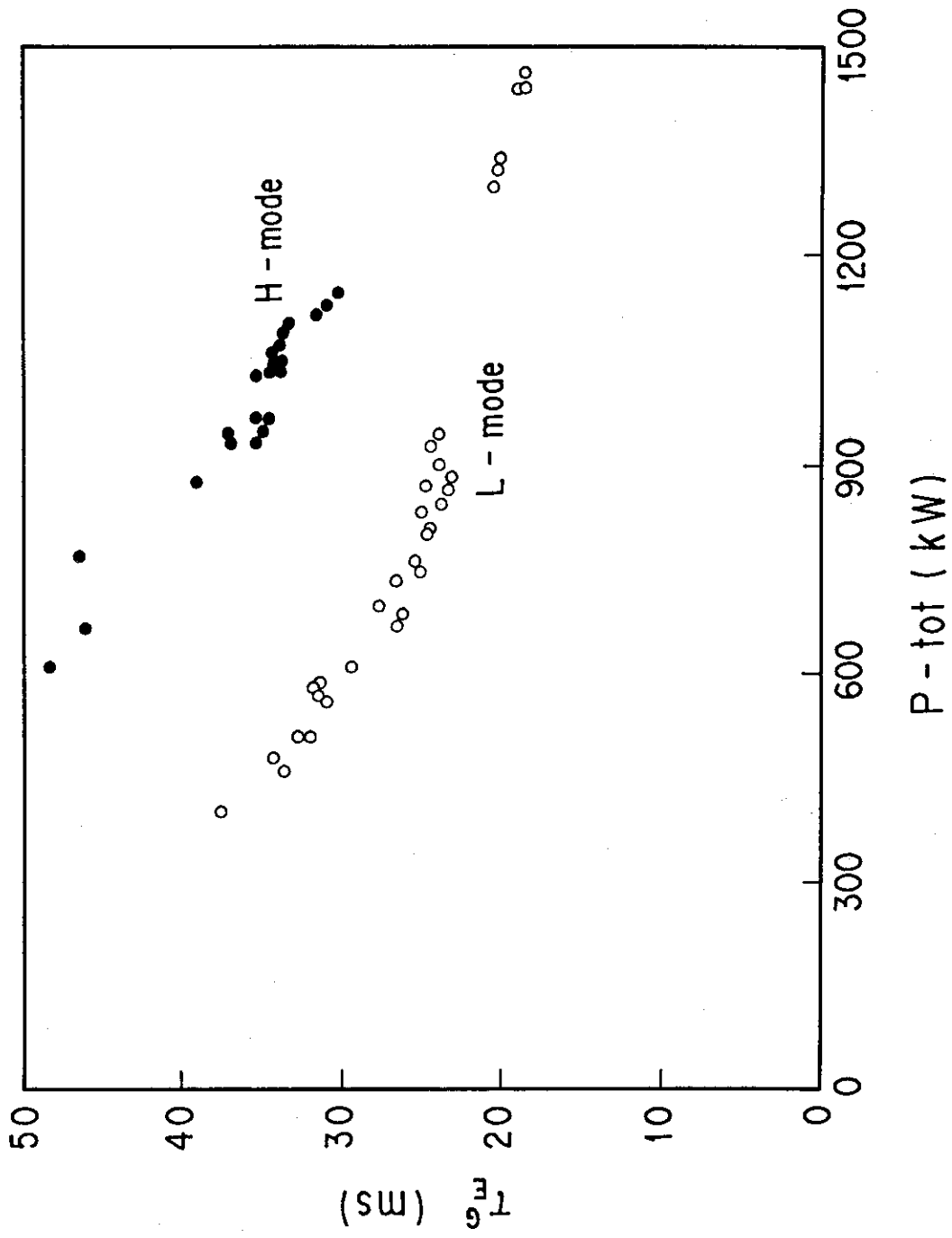
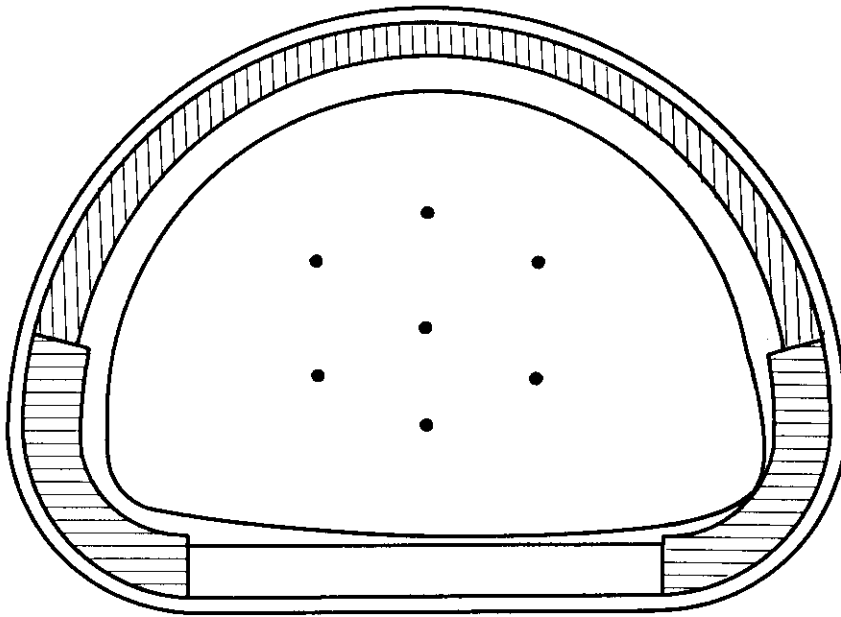


Fig.3 Global energy confinement time versus total energy input. Open circles are L-mode and solid circles are H-mode confinement times.

SHOT #28231



Double null Divertor

IP - CURRENT (KA)	275.2
R - AVERAGE (M)	1.302
Z - AVERAGE (M)	-0.004
R - INNER (M)	0.976
R - OUTER (M)	1.628
Rj	1.229
Zj	-0.001
α - HALF (M)	0.326
α - AVERAGE (M)	0.392
ELLIPTICITY	1.464
TRIANGULARITY	0.282
CROSS AREA (M**2)	0.482
VOLUME (M**3)	3.946
Q - SURF	4.576
BT (T)	1.177
BP+LI/2-1/2	0.318

Fig.4 Outermost magnetic surface of double null open divertor configuration.

#28231

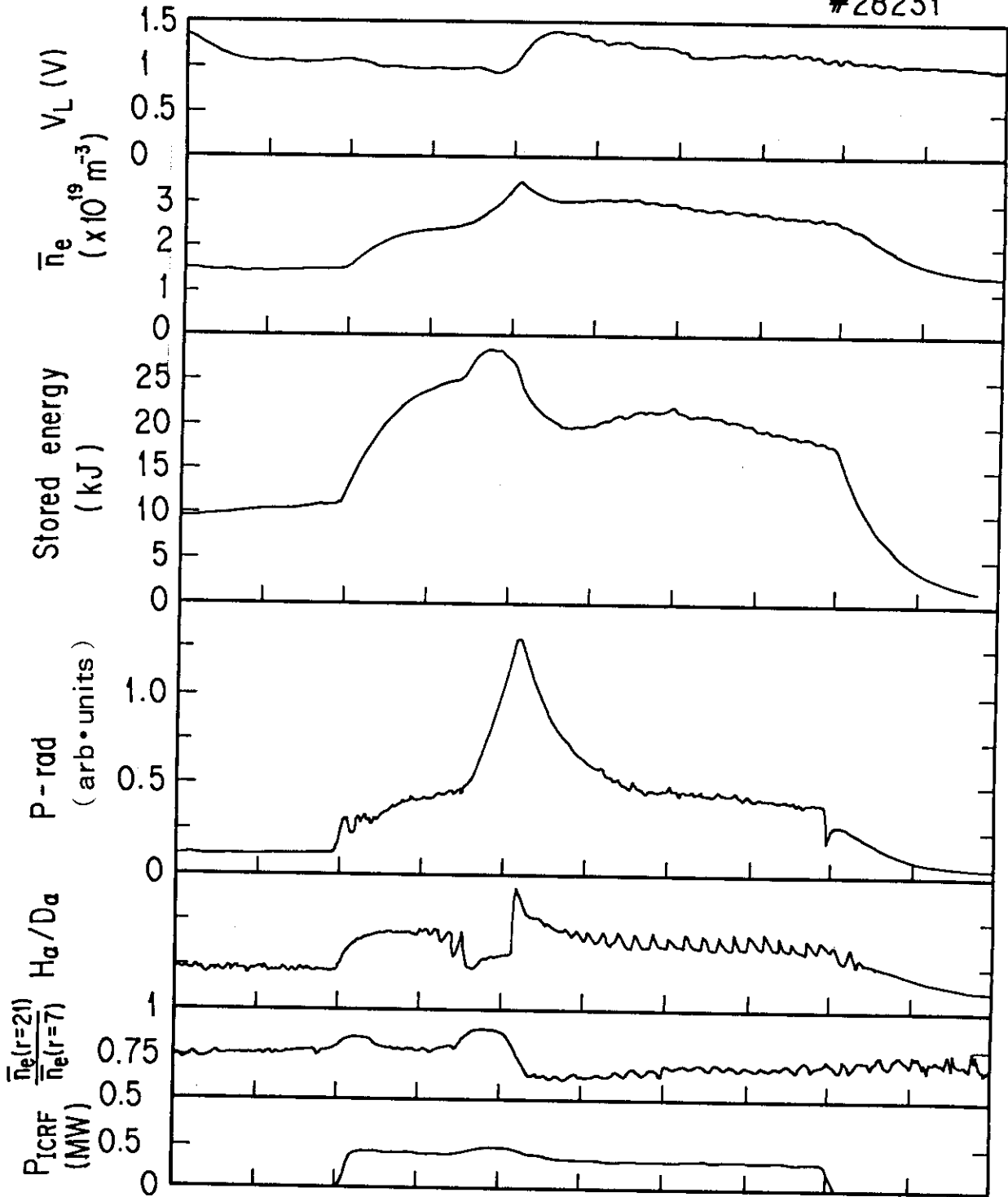
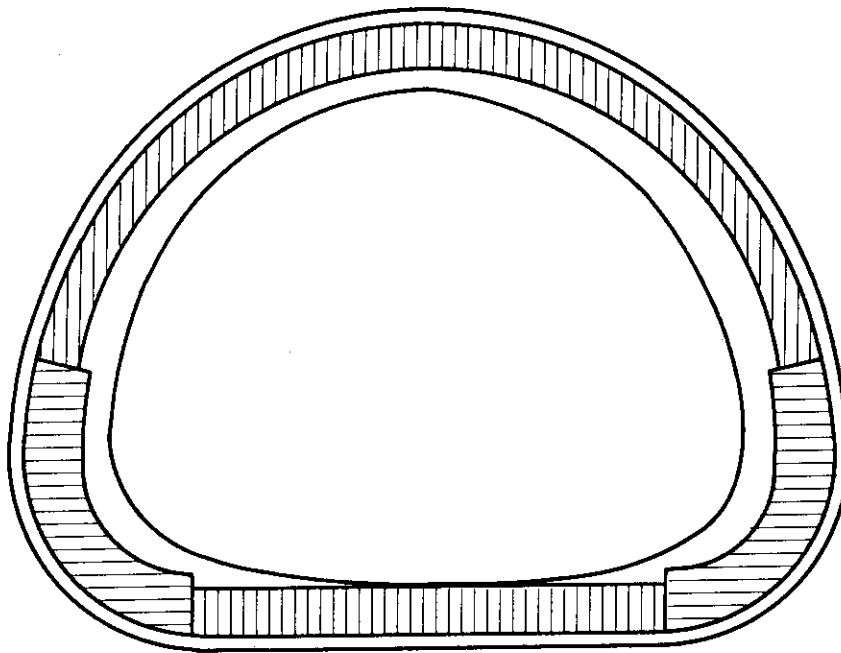


Fig.5 Time evolutions of double null open divertor configuration. From above, one turn loop voltage, line averaged electron density, plasma stored energy, radiation loss, $H\alpha/D\alpha$ emission, ratio of line averaged electron density at $R=151\text{cm}$ and $R=137\text{cm}$, and ICRF heating power.

SHOT #23810



D - shape Limiter

IP - CURRENT (KA)	334.2
R - AVERAGE (M)	1.296
Z - AVERAGE (M)	0.002
R - INNER (M)	0.959
R - OUTER (M)	1.632
Rj (M)	1.283
Zj (M)	0.006
A - HALF (M)	0.336
A - AVERAGE (M)	0.393
ELLIPTICITY	1.386
TRIANGULARITY	0.169
CROSS AREA (M**2)	0.485
VOLUME (M**3)	3.945
Q - SURF	2.921
BT (T)	1.109
BP + LI/2 - 1/2	0.242

Fig.6 Outermost magnetic surface of D-shape limiter discharge.

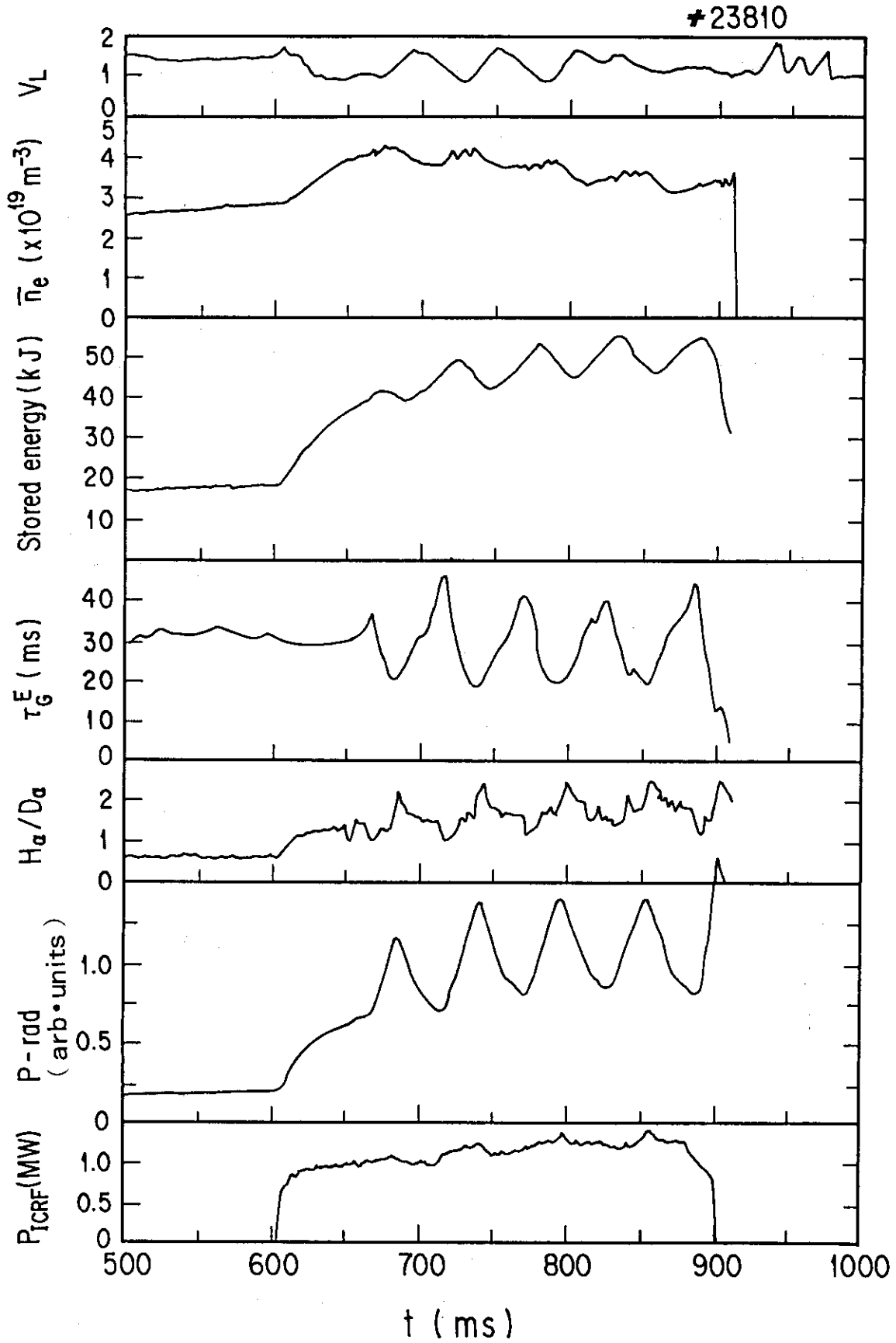


Fig.7 Time evolutions of D-shape limiter discharge. From above, one turn loop voltage, line averaged electron density, plasma stored energy, global energy confinement time, H_α/D_α emission, radiation loss, and ICRF heating power.

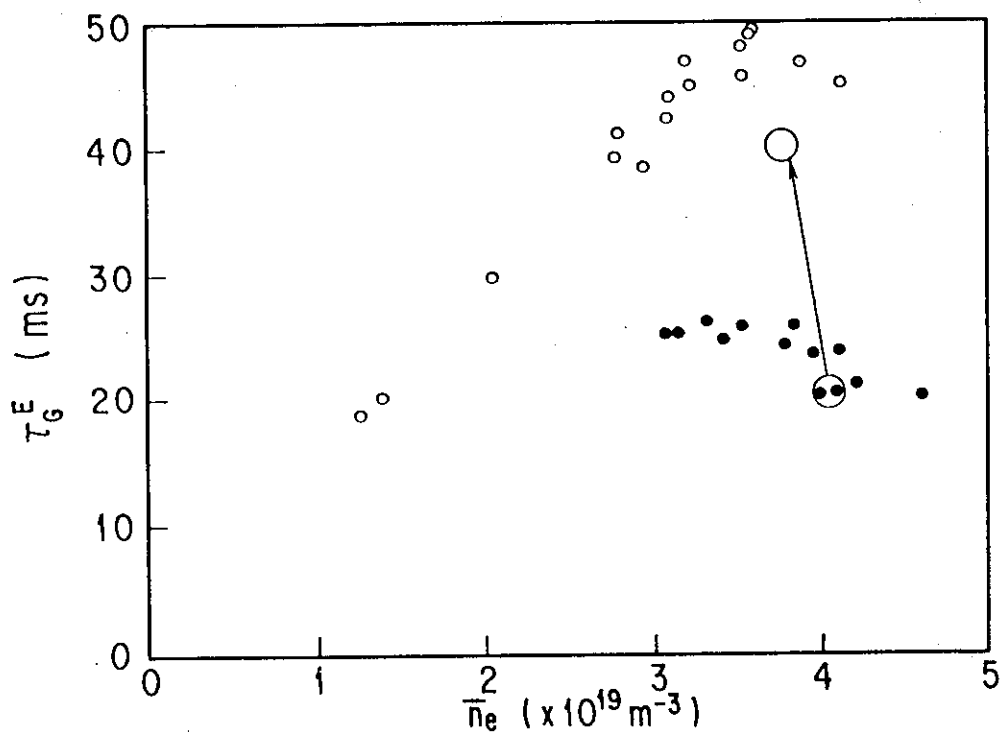


Fig.8(a) Density dependence of global energy confinement time. Open circles are ohmic and solid circles are L-mode ICRF heating results. Large open circles show the transient behavior during the transition.

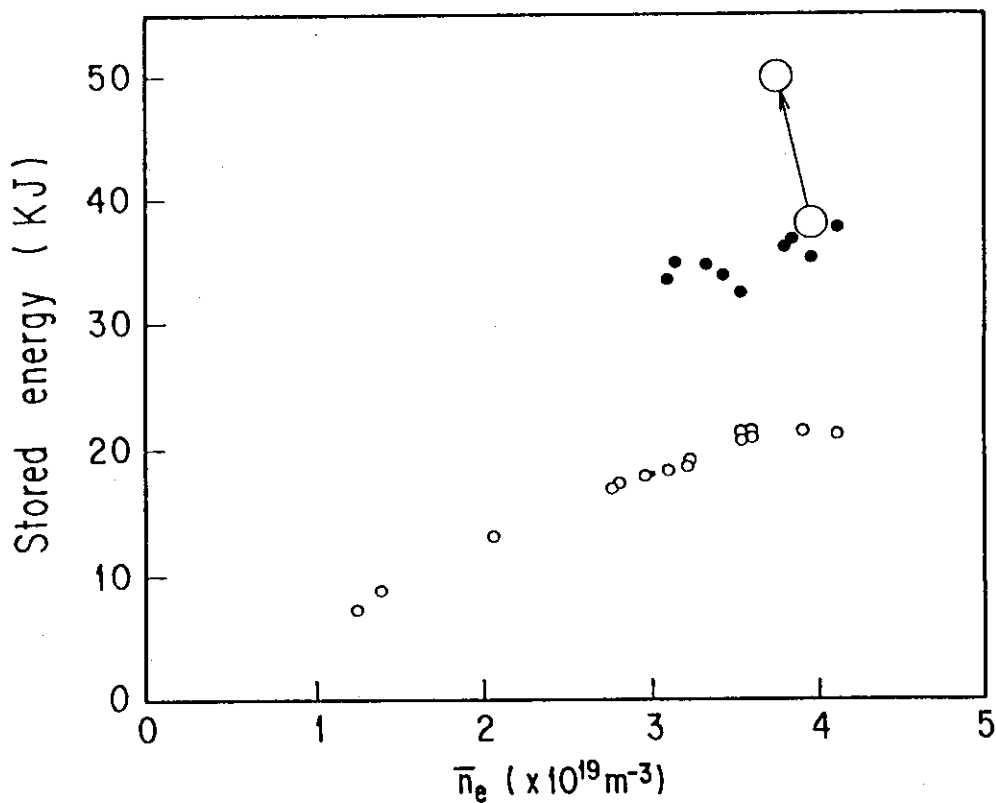


Fig.8(b) Density dependence of stored energy.

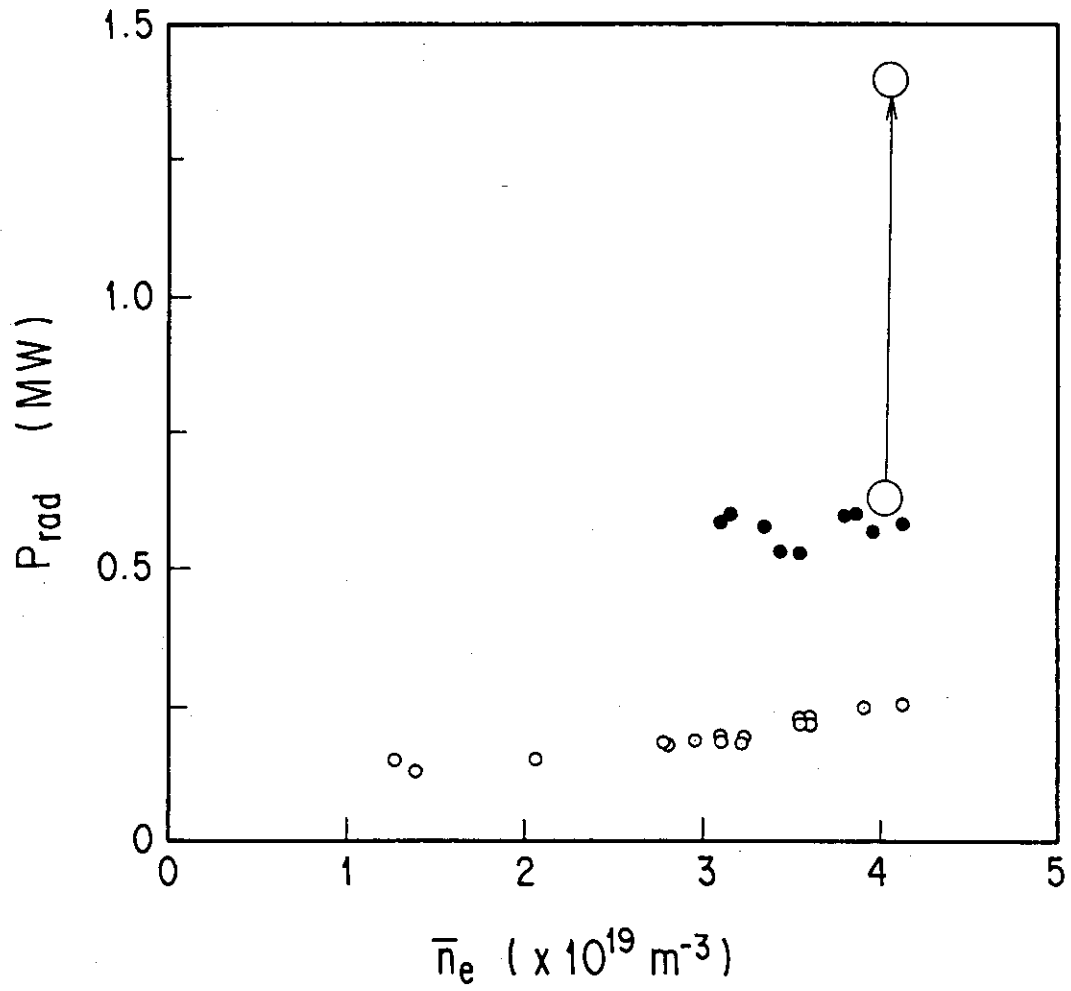


Fig.8(c) Density dependence of radiation loss.

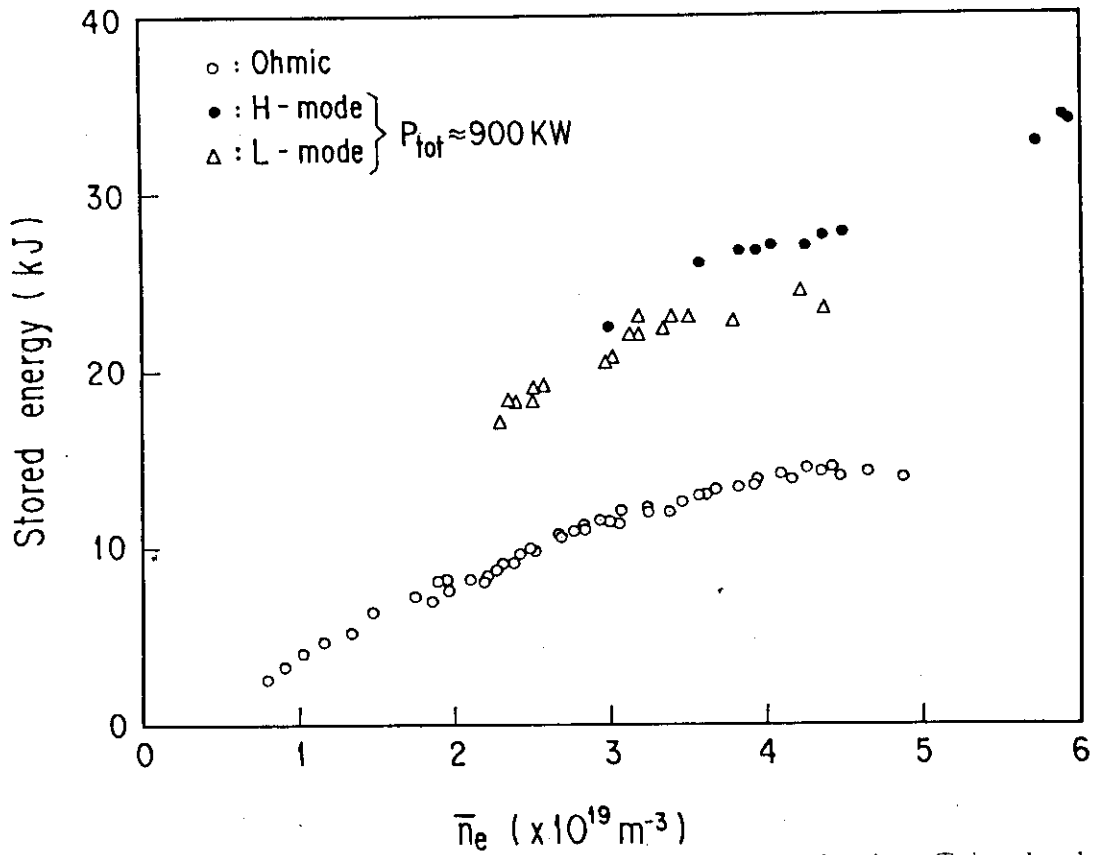


Fig.9 Stored energy is plotted against the line average electron density. Triangle show the energies of L-mode heating with the total heating power of 900 kw. Solid circles are of the H-mode heating with the same conditions as L-mode data. Open circles represent ohmic data.

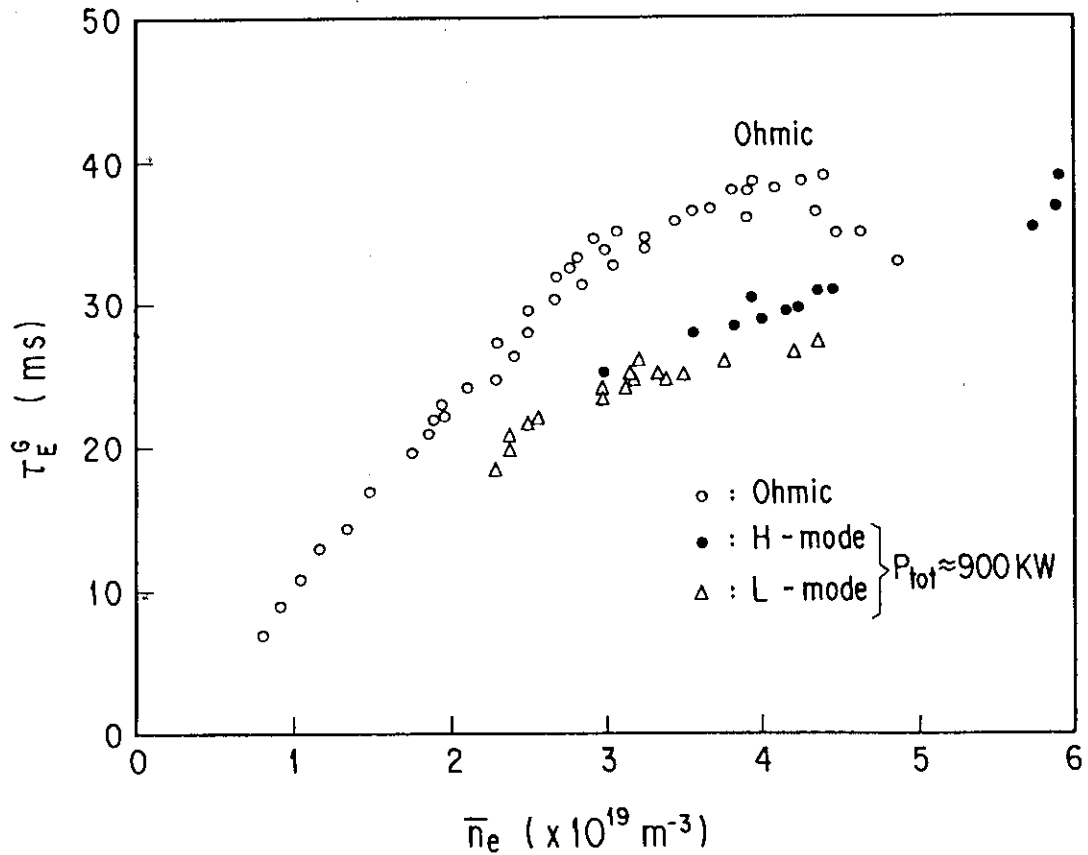


Fig.10 Replot of Fig.9 in terms of global energy confinement time.